Substitutional disorder and charge localization in manganites

Eduardo V Castro[1,2] and J M B Lopes dos Santos[1]

[1] CFP and Departamento de Física, Faculdade de Ciências Universidade do Porto,
P-4169-007 Porto, Portugal
[2] Instituto de Ciencia de Materiales de Madrid, CSIC, Cantoblanco, E-28049 Madrid, Spain

E-mail: evcastro@fc.up.pt and evcastro@icmm.csic.es

Abstract
In the manganites $RE_{1-x}AE_xMnO_3$ (RE and AE being rare-earth and alkaline-earth elements, respectively) the random distribution of RE^{3+} and AE^{2+} induces random, but correlated, shifts of site energies of charge carriers in the Mn sites. We consider a realistic model of this diagonal disorder, in addition to the double-exchange hopping disorder, and investigate the metal–insulator transition as a function of temperature, across the paramagnetic–ferromagnetic line, and as a function of doping x. Contrary to previous results, we find that values of parameters, estimated from the electronic structure of the manganites, are not incompatible with the possibility of a disorder-induced metal to insulator transition accompanying the ferromagnetic to paramagnetic transition at intermediate doping ($x \sim 0.2$–0.4). These findings indicate clearly that substitutional disorder has to be considered as an important effect when addressing the colossal magnetoresistance properties of manganites.

(Some figures in this article are in colour only in the electronic version)

1. Introduction

The discovery of colossal magnetoresistance (CMR) in the manganites $RE_{1-x}AE_xMnO_3$ (where RE and AE are trivalent rare-earth and divalent alkaline-earth ions, respectively) has attracted much interest to these perovskites [1–5]. On the one hand, understanding the origin of the CMR effect from a fundamental point of view is expected to give some insight into the complex behaviour seen in other strongly correlated systems, such as high-temperature superconductors. On the other hand, such a colossal response to an external perturbation still makes these Mn oxides very appealing from the point of view of applications [6]. This CMR effect, particularly 'colossal' in the so-called intermediate-bandwidth manganites for doping $x \sim 0.2$–0.4 [4], is intrinsically related to the presence of metallic behaviour below the Curie temperature (T_C) and insulating behaviour above it. Understanding the nature of this metal–insulator transition (MIT) accompanying the magnetic transition is thus a key point in the comprehension of the CMR effect.

Qualitatively, the correlation between transport and magnetic properties is well understood via Zener's double-exchange (DE) mechanism [7–9]: the spin of itinerant e_g and local t_{2g} Mn d electrons are aligned by Hund's rule; to lower the kinetic energy ferromagnetism is favoured, and at low temperature ($T < T_C$) a ferromagnetic half-metal is realized [1, 5]. Consequently, early proposals for the MIT focused on the random nature of hopping in the paramagnetic phase ($T > T_C$) [10–13]. Quantitative analysis based on the transfer matrix method showed concomitant ferro–paramagnetic and MITs for $x \sim 0.2$–0.4 when diagonal disorder is added to the DE model [14, 15]. The resultant CMR effect [16, 17], however, requires an amount of diagonal disorder that seems incompatible with potential fluctuations originated by the random distribution of RE^{3+} and AE^{2+} ions [5, 18]. This apparent failure of Anderson localization theories favoured models based on polaronic formation [19–21], owing to the electron–phonon coupling due to the Jahn–Teller effect in manganites [5]. It has been argued, however, that manganites fall into an intermediate electron–phonon coupling regime where small-polarons—key ingredients for an MIT driven by electron–phonon interactions—are hardly formed in the paramagnetic phase [5, 22]. More recent theories explain the CMR as an effect of competing orders: in brief, a ferromagnetic metal competes with a charge-ordered insulator phase, producing, for

$T \gtrsim T_C$, an inhomogeneous state highly sensitive to external perturbations where CMR is observed [23–29]. The underlying model producing such a phase-competition scenario takes into account, on the same footing, the DE mechanism and the electron–lattice coupling and, surprisingly, intrinsic disorder in manganites. Adding quenched disorder has been shown to make the inhomogeneous state even more sensitive to external perturbations, enhancing the CMR effect, and avoiding fine tuning of model parameters [30]. However, the need to include disorder on the same level as the DE mechanism and coupling to Jahn–Teller phonons strongly contradicts the observation that disorder in manganites is sufficiently weak for a virtual crystal approximation to be reasonable [5, 18].

In this paper we consider a realistic model for diagonal (substitutional) disorder in manganites, in addition to the DE hopping disorder, and investigate the MIT as a function of temperature, across the paramagnetic–ferromagnetic line, and as a function of doping x. Contrary to previous results [5], we find that values of parameters, estimated from the electronic structure of manganites [18, 31], are not incompatible with the possibility of a disorder-induced MIT accompanying the ferromagnetic to paramagnetic transition at intermediate doping ($x \sim 0.2$–0.4). Therefore, substitutional disorder has to be considered at least on the same footing as the coupling to the lattice when addressing the CMR properties of manganites. These findings give support to theories where disorder is a key ingredient [32], as the phase-competition scenario for CMR, where, as mentioned above, diagonal disorder plays a crucial role [23–30].

2. The model

In order to model substitutional disorder in manganites we note that, for each carrier introduced in the system, there is an $RE^{3+} \rightarrow AE^{2+}$ substitution. The corresponding change in the Coulomb field shifts the site energy of an electron in a manganese site at a distance R by

$$V(R) = \frac{e^2}{4\pi\varepsilon_0 \varepsilon R}, \tag{1}$$

where ε is the relative dielectric constant of the material. We can take this effect into account by including a random site energy term in the DE Hamiltonian:

$$H = -\sum_{\langle ij\rangle}(t(\mathbf{S}_i,\mathbf{S}_j)c_i^\dagger c_j + \text{h.c.}) + \sum_i \epsilon_i c_i^\dagger c_i. \tag{2}$$

The first term on the right-hand side in (2) is the usual infinite Hund coupling DE Hamiltonian, where the hopping of e_g electrons between nearest-neighbours Mn sites depends on the background configuration of classical t_{2g} core spins $\mathbf{S}_i = S(\sin\theta_i \cos\phi_i, \sin\theta_i \sin\phi_i, \cos\theta_i)$, with

$$t(\mathbf{S}_i,\mathbf{S}_j) = t[\cos(\theta_i/2)\cos(\theta_j/2) + e^{-i(\phi_i-\phi_j)}$$
$$\times \sin(\theta_i/2)\sin(\theta_j/2)]. \tag{3}$$

The second term on the right-hand side of (2) stands for the diagonal site disorder. It has been modelled in previous works with a uniform probability distribution for $-W/2 \leqslant \epsilon_i \leqslant W/2$

(Anderson disorder) [14–16]. Through the analysis of the mobility edge trajectory in the energy versus disorder (W) plane, obtained using the transfer matrix method [33–35], it has been found that an MIT occurs when the system crosses the ferro–paramagnetic transition line, for $0.2 < x < 0.5$, provided the diagonal disorder is strong enough, $12t < W < 16.5t$. The plausibility of such a large value of the disorder parameter, however, has been questioned [5] mainly on the basis of density functional results obtained by Pickett and Singh [18, 31]. In the following we show that a thorough analysis of the results of [18] and [31] are, in fact, not incompatible with disorder in the range $12t < W < 16.5t$.

2.1. Substitutional disorder strength

Pickett and Singh [18, 31] looked at the $x = 1/3$ concentration and performed LDA calculations of band structure for a periodic structure of $La_2CaMn_3O_9$ with a tetragonal unit cell containing an La–Ca–La set of planes. There are two inequivalent Mn sites in this structure, one with eight La^{3+} and the other with four Ca^{2+} and four La^{3+} nearest neighbours (NNs). The local density of states at the Mn sites showed a difference of $\Delta\epsilon_{Mn} \approx 0.5$ eV between the band edges for these two types of sites, which was interpreted as arising from the different charges Ca^{2+} and La^{3+}. Thus, $\Delta\epsilon_{Mn} = 4V_1$ with V_1 given by (1) with $R = a\sqrt{3}/2$ (the first NN La–Mn distance):

$$V_1 = \frac{2e^2}{\sqrt{3}\pi\varepsilon_0\varepsilon a}, \tag{4}$$

where $a \approx 3.9$ Å is the Mn–Mn distance [36]. From the calculated value of $\Delta\epsilon_{Mn}$ a dielectric constant $\varepsilon \approx 34$ is obtained, or equivalently $V_1 \approx 0.13$ eV $\approx 0.6t$ ($t \approx 0.2$ eV was used [4]).

Such a dielectric constant, however, is quite unlikely. We should note that equation (4) is actually a microscopic description, where $R = a\sqrt{3}/2 \approx 3.4$ Å. Neglecting metallic screening, we should get a relative permittivity reflecting the polarizability of the Mn d–O p complex, as pointed out in [18]. Infrared reflectivity measurements on $La_{0.67}Ca_{0.33}MnO_3$ give a high-frequency dielectric constant $\varepsilon_\infty \approx 7.5$ at 78 K [37] which, though being only a lower bound, casts serious doubts on $\varepsilon \approx 34$. On the other hand, note that the result $\Delta\epsilon_{Mn} = 4V_1$ is a special case where only the first NNs (La/Ca sites) contribute to the local potential. A more realistic situation should account for the next NNs' contributions.

It is easy to generalize the first NN result $\Delta\epsilon_{Mn} = 4V_1$ in order to account for the Coulomb contribution of the ith shell, $V_i = e^2/(4\pi\varepsilon_0\varepsilon_i R_i)$, where ε_i is the dielectric constant for the given shell. In particular, taking into account second-and third-NNs, we get $\Delta\epsilon_{Mn} = 4V_1 - 12V_3$, where V_2 is absent because the two inequivalent Mn sites have the same second-NN environment. The value $\Delta\epsilon_{Mn} \approx 0.5$ eV found by Pickett and Singh [18] is reproduced with $\varepsilon_1 \approx 10$ and $\varepsilon_3 \approx 17$, where we used $R_3 = a\sqrt{19}/2 \approx 8.5$ Å. Following [18], we will keep only first-and second-NN contributions, with $\varepsilon_1 = \varepsilon_2 \approx 10$, and $R_2 = a\sqrt{11}/2 \approx 6.5$ Å. The resulting random site energies may be written as
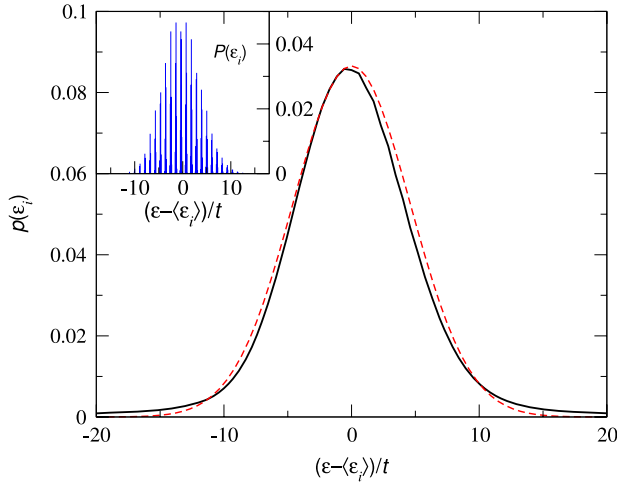
$$\epsilon_i = V_1(l_{i1} + l_{i2}\sqrt{3/11}), \tag{5}$$

Figure 1. The full line shows the probability distribution of Mn site energies due to random placement of RE^{3+} (2/3 probability) and AE^{2+} (1/3 probability) on first-and second-nearest-neighbour sites, obtained by substituting δ functions in (6) by Lorentzians with half-width t at half-maximum. A dielectric constant of $\varepsilon \approx 10$ was used for both shells. The dashed line is the fit to the full line with a Gaussian distribution. The inset shows the true discrete Mn-site energy probability.

where l_{ij} is the number of AE^{2+} ions in the jth shell of Mn site i for a given RE^{3+}/AE^{2+} configuration. Inserting $\varepsilon_1 \approx 10$ in equation (4) we get $V_1 \approx 0.43$ eV $\approx 2.1t$. The probability distribution for this random, but correlated, site energy model may be written as

$$p(\epsilon_i) = \sum_{l_{i2}=0}^{24} \binom{24}{l_{i2}} \sum_{l_{i1}=0}^{8} \binom{8}{l_{i1}} x^{l_{i1}+l_{i2}}$$
$$\times (1-x)^{32-l_{i1}-l_{i2}} \delta\left[\epsilon_i - V_1\left(l_{i1} + l_{i2}\frac{\sqrt{3}}{\sqrt{11}}\right)\right]. \quad (6)$$

In figure 1 we show the resulting coarse-grained distribution as a function of $\epsilon_i - \langle\epsilon_i\rangle$ for $x = 1/3$, where the average site energy is $\langle\epsilon_i\rangle = xV_1(8 + 24\sqrt{3/11})$; the inset shows the true discrete Mn-site energy probability, as given by the weight of the delta functions in equation (6). The distribution is approximately Gaussian with a root mean square (RMS) deviation:

$$\sigma \equiv \sqrt{\langle\epsilon_i^2\rangle - \langle\epsilon_i\rangle^2} \simeq 4.6t, \quad (7)$$

as obtained by fitting with a Gaussian distribution (dashed line in figure 1). A rectangular distribution with the same RMS deviation has $W = \sigma\sqrt{12} \approx 15.9t$; well in the range required for an MIT at T_C, $12t < W < 16.5t$ [15, 17]. The effect on T_C of a discrete random site energy distribution similar to equation (6), but restricted to the NN shell, has been considered in [38].

The analysis which lead us to figure 1 and equation (7) was previously carried out in [18], but with a very different conclusion about the strength of disorder in CMR manganites. The main difference with respect to the present analysis is the value of the dielectric constant entering equation (6) through

V_1[3]. Even though it is stated in [18] that first and second shells of RE^{3+}/AE^{2+} sites are taken into account with $\varepsilon_1 = \varepsilon_2 \approx 10$, we can only reproduce figure 1 of [18] (the analogue of our figure 1) if equation (6) is used with $\varepsilon_1 = \varepsilon_2 \approx 34$ (an unlikely dielectric constant, as discussed above). As a consequence, the associated distribution was found to have an RMS of $\sigma \approx 1.3t \approx 0.26$ eV[4]. This means that a rectangular distribution with the same RMS deviation has $W = \sigma\sqrt{12} \approx 4.5t$; well below the values required for an MIT at T_C, $12t < W < 16.5t$ [15, 17].

3. Results and discussion

From the above considerations we may conclude that a realistic parametrization of diagonal disorder is mandatory for a precise estimate of the effect of substitutional disorder in manganites. We have performed a transfer matrix calculation [33–35] using the model given in equation (2), with site energies calculated from a random distribution of the dopant ions AE^{2+}. The first and second shells of RE^{3+}/AE^{2+} sites were taken into account assuming equal dielectric constants, which results in random on-site energies given by (5) and a site energy distribution given by (6). In this case the site disorder is parametrized by x, which determines the fraction of AE^{2+} ions in the system and thus the variables l_{ij} in equation (5), and by the parameter V_1 given in equation (4), or equivalently the dielectric constant ε. The doping level x also determines the Fermi energy in the system, which was calculated by integrating over the disorder-averaged density of states obtained for clusters of $64 \times 64 \times 64$ sites using the recursive Green's function method [39].

The transfer matrix technique gives reliable information about the extended or localized nature of the eigenstates [35, 40]. For a quasi-one-dimensional system with length L and cross section $M \times M$, where $L \gg M$ (in units of the lattice constant), the method provides the localization length λ_M of the finite system from the smallest Lyapunov exponent of the respective transfer matrix product. The scaling behaviour of the normalized finite-size localization length λ_M/M then determines the nature of the eigenstates for a given x and V_1 at the Fermi energy. Extended (localized) states show increasing (decreasing) λ_M/M as M increases. This behaviour can be appreciated in the inset of figure 2 for $x = 0.30$ in the paramagnetic phase, where the direction of each spin is chosen randomly from a uniform distribution on a sphere. We have used system bars ($L \times M \times M$) with a longitudinal length L such that the relative error in λ_M is $\lesssim 1\%$ (typically $L \sim 10^5$) and $M = 6, 8, 10, 12$. At criticality λ_M/M is independent of M, signalling the Anderson transition, and providing the critical parameter values [41].

The main result of this work is presented in figure 2. For each concentration the critical values of V_1, at which

---

[3] An additional difference comes from the misplaced second shell of RE^{3+}/AE^{2+} sites in [18]. The distances to the first and to the second shells differ by 48%, and not by the referred-to 13% in [18]. This error, however, does not change considerably the results: while in the case of 48% difference the second shell has 24 sites, in the case of 13% difference it has only 6 sites.

[4] In [18] the full width of the distribution at half-maximum was found to be $\delta\epsilon \approx 0.6$ eV. If we assume the distribution to be Gaussian, the full width at half-maximum is related to the root mean square σ as $\delta\epsilon = \sigma 2\sqrt{2\ln 2}$.
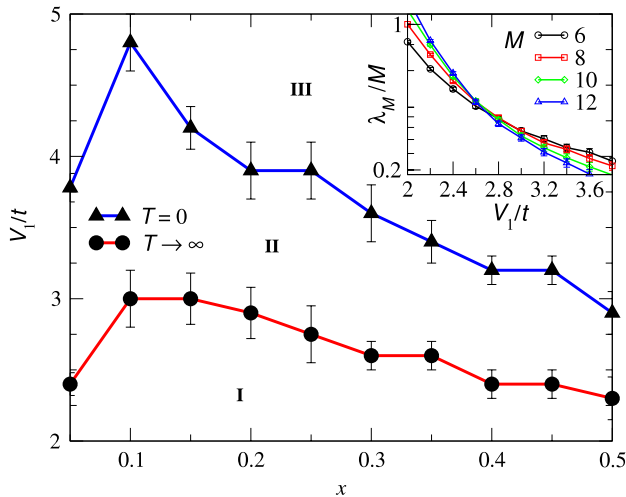
Figure 2. Critical value of V_1 versus x in the paramagnetic (circles) and ferromagnetic phases (triangles). A system with (x, V_1) in region **I (III)** is metallic (insulator) in the paramagnetic and ferromagnetic phases; in region **II** the mobility edge crosses the Fermi level in the para–ferromagnetic transition. The inset shows the typical behaviour of the normalized finite-size localization length λ_M/M versus V_1/t across the MIT for the particular case of $x = 0.30$ in the paramagnetic phase.

the mobility edge and the Fermi level coincide, were calculated in the paramagnetic (circles) and ferromagnetic phases (triangles). A value of V_1 between these two (i.e. in region **II**) implies a crossing of the Fermi level and the mobility edge when the system orders magnetically. A value of $V_1 \approx 3t$ is sufficient to give rise to an Anderson MI transition for concentrations $x \sim 0.2$–0.5. While it is still higher than the estimate based on [18] and [31], $V_1 \approx 2.1t$, it is sufficiently close to cast some doubt on a straightforward dismissal of a role of Anderson localization in the magnetoresistance of the manganites. Moreover, the value $V_1 \approx 2.1t$ only takes into account the random distribution of potential sources, namely RE^{3+} and AE^{2+} ions. The presence of RE/AE ionic size mismatch is expected to enhance considerably the disorder effects [42–44]. Note also that, in this model, the critical value of disorder does not vary monotonically with x and shows a maximum at around $x \sim 0.1$. One should bear in mind that, in this model, changing x also changes the distribution of site energies (equation (6)), and so V_1 does not, by itself, characterize the disorder.

A final remark regarding the relevance of the model used in this work is in place. The model given by equation (2) with correlated on-site disorder as in (5) is certainly incomplete: it neglects electron–lattice coupling, orbital degrees of freedom, anti-ferromagnetic exchange between localized t_{2g} spins and electron–electron interactions between e_g electrons. Consequently, it does not distinguish between the three main manganite groups (large, intermediate and low bandwidth) and cannot reproduce many of the complex phases appearing in each of their phase diagrams [4]. However, it is general enough and not tremendously complex to address the question of how important is substitutional disorder in manganites; this is the motivation for using it.

4. Conclusions

We have shown that a careful analysis of the Mn-site energies arising from a random distribution of AE^{2+} and RE^{3+} ions in manganites produce a probability distribution with an RMS deviation $\sigma \approx 4.6t$. This RMS is a consequence of a parametrization of screened Coulomb energies for which an energy shift $V_1 \approx 2.1t$ is assumed to show up in an Mn site whenever an NN replacement $RE^{3+} \rightarrow AE^{2+}$ occurs. Such an RMS value already places the system in the disorder window for which an MIT occurs when the ferro–paramagnetic transition takes place. We have developed a DE model with realistic parametrization of on-site disorder which shows it undergoes an MIT at the ferro–paramagnetic transition for $V_1 \approx 3t$. This V_1 value is slightly larger than the expected $V_1 \approx 2.1t$, but it is sufficiently close to unveil the importance of substitutional disorder in manganites and show that disorder must be considered, at least on the same footing as the coupling to the lattice. These findings give support to theories where disorder is a key ingredient [32], as the phase-competition scenario for CMR, where diagonal disorder has been found to play a crucial role [23–30]. Such a key role played by disorder was also recently observed in a series of experiments in half-doped manganites [45, 46], where A-site ordered and disordered systems have been successfully prepared and compared.

Acknowledgments

References

[1] Coey J M D, Viret M and Von Molnar S 1999 *Adv. Phys.* **48** 167–293
[2] Loktev V M and Pogorelov Y G 2000 *Low Temp. Phys.* **26** 171–93
[3] Salamon M B and Jaime M 2001 *Rev. Mod. Phys.* **73** 583–628
[4] Dagotto E, Hotta T and Moreo A 2001 *Phys. Rep.* **344** 1–153
[5] Edwards D M 2002 *Adv. Phys.* **51** 1259–318
[6] Dagotto E 2005 *Science* **309** 257–62
[7] Zener C 1951 *Phys. Rev.* **82** 403–5
[8] Anderson P W and Hasegawa H 1955 *Phys. Rev.* **100** 675–81
[9] de Gennes P G 1960 *Phys. Rev.* **118** 141–54
[10] Kogan E M and Auslender M I 1988 *Phys. Status Solidi* b **147** 613–20
[11] Auslender M I, Kogan E M and Tretyakov S V 1988 *Phys. Status Solidi* b **148** 289–95
[12] Varma C M 1996 *Phys. Rev.* B **54** 7328–33
[13] Kogan E, Auslender M and Kaveh M 1999 *Eur. Phys. J.* B **9** 373–6
[14] Li Q, Zang J, Bishop A R and Soukoulis C M 1997 *Phys. Rev.* B **56** 4541
[15] Sheng L, Xing D Y, Sheng D N and Ting C S 1997 *Phys. Rev.* B **56** R7053–6
[16] Sheng L, Xing D Y, Sheng D N and Ting C S 1997 *Phys. Rev. Lett.* **79** 1710–3
[17] Zaránd G, Moca C P and Jankó B 2005 *Phys. Rev. Lett.* **94** 247202
[18] Pickett W E and Singh D J 1997 *Phys. Rev.* B **55** R8642–5

[19] Millis A J, Littlewood P B and Shraiman B I 1995 *Phys. Rev. Lett.* **74** 5144–7

[20] Millis A J, Shraiman B I and Mueller R 1996 *Phys. Rev. Lett.* **77** 175–8

[21] Röder H, Zang J and Bishop A R 1996 *Phys. Rev. Lett.* **76** 1356–9

[22] Bozin E S, Schmidt M, DeConinck A J, Paglia G, Mitchell J F, Chatterji T, Radaelli P G, Proffen T and Billinge S J L 2007 *Phys. Rev. Lett.* **98** 137203

[23] Moreo A, Mayr M, Feiguin A, Yunoki S and Dagotto E 2000 *Phys. Rev. Lett.* **84** 5568–71

[24] Burgy J, Mayr M, Martin-Mayor V, Moreo A and Dagotto E 2001 *Phys. Rev. Lett.* **87** 277202

[25] Burgy J, Moreo A and Dagotto E 2004 *Phys. Rev. Lett.* **92** 097202

[26] Motome Y, Furukawa N and Nagaosa N 2003 *Phys. Rev. Lett.* **91** 167204

[27] Motome Y, Furukawa N and Nagaosa N 2005 *Lecture Notes in Physics* vol 678, ed M Donath and W Nolting (Berlin: Springer) p 71

[28] Kumar S and Majumdar P 2006 *Phys. Rev. Lett.* **96** 016602

[29] Sen C, Alvarez G and Dagotto E 2007 *Phys. Rev. Lett.* **98** 127202

[30] Sen C, Alvarez G, Aliaga H and Dagotto E 2006 *Phys. Rev. B* **73** 224441

[31] Pickett W E and Singh D J 1996 *Phys. Rev. B* **53** 1146–60

[32] Narimanov E E and Varma C M 2001 *Phys. Rev. B* **65** 024429

[33] Mackinnon A and Kramer B 1981 *Phys. Rev. Lett.* **47** 1546–9

[34] Mackinnon A and Kramer B 1983 *Z. Phys. B* **53** 1–13

[35] Kramer B and MacKinnon A 1993 *Rep. Prog. Phys.* **56** 1469–564

[36] Coey J M D, Viret M, Ranno L and Ounadjela K 1995 *Phys. Rev. Lett.* **75** 3910–3

[37] Boris A V, Kovaleva N N, Bazhenov A V, van Bentum P J M, Rasing T, Cheong S W, Samoilov A V and Yeh N C 1999 *Phys. Rev. B* **59** R697–700

[38] Salafranca J and Brey L 2006 *Phys. Rev. B* **73** 214404

[39] Haydock R 1980 *Solid State Physics* vol 35, ed H Ehrenreich, F Seitz and D Turnbull (New York: Academic) p 215

[40] Slevin K and Ohtsuki T 1999 *Phys. Rev. Lett.* **82** 382–5

[41] Xiong S J, Xing D Y, Evangelou S N and Sheng D N 2003 *Phys. Lett.* A **311** 426–31

[42] Sheng L, Sheng D N and Ting C S 1999 *Phys. Rev. B* **59** 13550–3

[43] Alonso J L, Fernandez L A, Guinea F, Laliena V and Martin Mayor V 2002 *Phys. Rev. B* **66** 104430

[44] Kumar S and Kampf A P 2008 *Phys. Rev. Lett.* **100** 076406

[45] Akahoshi D, Uchida M, Tomioka Y, Arima T, Matsui Y and Tokura Y 2003 *Phys. Rev. Lett.* **90** 177203

[46] Mathieu R, Akahoshi D, Asamitsu A, Tomioka Y and Tokura Y 2004 *Phys. Rev. Lett.* **93** 227202